

LiFi for Industry 4.0: Main Features, Implementation and Initial Testing of IEEE Std 802.15.13

Kai Lennert Bober*, MEMBER, IEEE, Anselm Ebmeyer*, Falko Dressler†, Fellow, IEEE, Ronald Freund*†, MEMBER, IEEE, Volker Jungnickel*†, MEMBER, IEEE

¹* Fraunhofer Heinrich Hertz Institute, Einsteinufer 37, 10587 Berlin, Germany

† Technical University of Berlin, Einsteinufer 25, 10587 Berlin, Germany

(Invited Paper)

CORRESPONDING AUTHOR: Lennert Bober (e-mail: bober@ieee.org).

This work was supported by the German Federal Ministry for Economic Affairs and Climate Action in the project LINCNET (01MT22001B) and the German Ministry of Digital and Transport in the project 5G-COMPASS (19OI22017A).

ABSTRACT As industrial communication continues to evolve to increase flexibility through wireless communication, networked optical wireless communication (OWC), also known as LiFi, has emerged as a promising candidate technology due to its unlicensed spectrum and relatively deterministic propagation. The inherent containment of light improves security, enables dense cellular networks with spatial reuse, and results in reduced sporadic interference while providing high-capacity short range communication links to mobile end devices. This paper outlines the features of the new IEEE Std 802.15.13-2013, suitable for industrial OWC, and presents details of our prototype implementation along with initial experiments. The standard specifies deterministic medium access control (MAC), based on dynamic time division multiple access (TDMA), as well as two physical layers (PHYs) for extended range and robustness, and for spectral efficiency, respectively. Our prototype includes a central coordinator, implemented entirely in software, running on commodity server hardware. It connects to distributed ceiling-mounted optical wireless frontends via a packet-switched network (Ethernet) and is capable of forming them into adaptive virtual cells on a per-user basis. This approach enhances reliability through multiple-input multiple-output (MIMO) transmission and allows for smooth mobility. We implemented the Pulsed Modulation PHY (PM-PHY) on a commercially available field programmable gate array (FPGA) evaluation board. Initial test results indicate that the PM-PHY supports typical distances of up to 6 m between the ceiling and the mobile device. The MAC achieves deterministic latency values below 4 ms.

INDEX TERMS Optical Wireless Communication, OWC, IEEE Std 802.15.13, Industrial Networks, LiFi, VLC, DPDK, FPGA, TSN

I. Introduction

NETWORKED optical wireless communication (OWC), also known as LiFi, is considered a potential building block for future wireless industrial networks. This is due to its potential for very dense deployments, enhanced confidentiality, robustness to jamming, and license-free operation. It was shown that a robotic manufacturing cell can be illuminated by multiple optical frontends (OFEs) allowing the arm of a mobile robot to be reliably connected via light

and move freely within the cell [1]. Extending that concept, a ceiling-mounted wireless infrastructure has been proposed to expand coverage to larger areas with LiFi. It provides a dense wireless network and supports deterministic wireless communication between the fixed in-building network infrastructure and mobile devices in the service area [2].

Parallel work has shown that precise indoor positioning and sensing can be realized as new services based on the communication capabilities of a LiFi system. Unlike radio

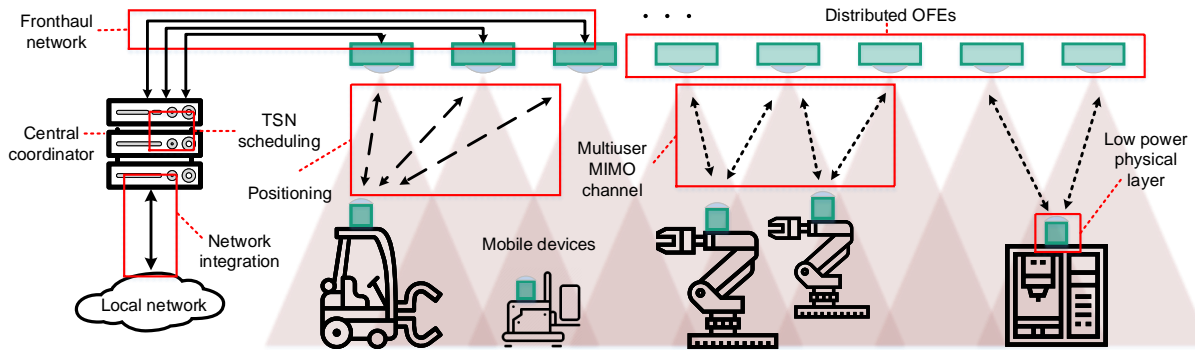


FIGURE 1. Vision of a LiFi infrastructure based on ceiling-mounted optical frontends (OFEs) delivering dense wireless access in industrial environments. Different end devices, such as robots in a flexible manufacturing cell, automated guided vehicles (AGVs), or handheld devices can be connected wireless with a high quality of service (QoS) [2].

waves, light propagates primarily via the line-of-sight. Time-of-flight measurements (also known as ranging or timing advance) between the mobile device and multiple OFEs, together with super-resolution based on channel state information (CSI) used for fine timing and multilateration, can overcome practical issues of received signal-strength (RSS) based positioning approaches with fingerprinting. In this way, 3D indoor positioning with 3 cm accuracy has been demonstrated for the first time [3]. Note that both reliable low-latency communication and precise positioning/sensing can be realized with the same LiFi infrastructure proposed for Industry 4.0. Fig. 1 illustrates our vision of the industrial wireless LiFi network originally described in [2].

Current radio technologies, especially when using shared spectrum, are usually not capable of providing these advanced characteristics to the degree that is needed for future factory automation. To make LiFi suitable for industrial wireless applications, it must ensure reliable transmissions with zero packet loss and support timely forwarding of data by minimizing delay and delay variation (“jitter”). However, no affordable off-the-shelf wireless protocol is available to exploit the full potential of LiFi in industrial applications.

5G protocols can, in principle, be operated transparently over the light channel. However, the ideally required routines are neither fully specified nor implemented in the latest releases of the 5G standard. Moreover, 5G equipment is costly and its deployment only manageable by 5G experts.

There have been recent standardization activities for LiFi resulting in the International Telecommunication Union Telecommunication Standardization Sector (ITU-T) Recommendation G.9991 [4], which introduces orthogonal frequency-division multiplex (OFDM) with adaptive bitloading and a selective repeat mechanisms to improve reliability. However, the standard uses a contention-based medium access protocol to achieve high throughput and handles interference from other access points by sharing the spectrum in the time domain. These mechanisms cause latency variations (“jitter”) and increase average latency, which is not suitable to support real-time transmission.

The IEEE Std 802.11bb-2023 [5] can be implemented using existing Wi-Fi chipsets designed for home and enterprise applications. It is based on the well-known listen-before-talk protocol, in which multiple access points and stations share the channel in the time domain. In a heterogeneous device environment where devices with legacy and new chipsets are used, channel access has a random element and is not deterministic. This is in contrast to the high reliability, low-latency, and low-jitter requirements for Industry 4.0.

Consequently, the IEEE 802.15.13 task group defined OWC to integrate with IEEE 802 local area networks (LANs) as a transparent sub-network with the goal of supporting modern time-sensitive networking (TSN) mechanisms for real-time applications. Additionally, the IEEE Std 802.15.13 specifies distributed multiple-input multiple-output (D-MIMO) to overcome potential packet loss and the corresponding latency associated with handover from one access point to the next. Handovers between cells are handled at the physical layer and replaced by multiple-input multiple-output (MIMO) schemes similar to “antenna selection,” based on CSI feedback obtained from the mobile devices. The MAC layer supports deterministic channel access based on dynamic time division multiple access (TDMA), in which contention-free slots are allocated to each mobile device. To minimize jitter, control and management frames can be scheduled adaptively in slots that are not required by time-sensitive streams. The standard supports two physical layers (PHYs), i.e., OFDM with adaptive bitloading and on-off-keying (OOK) with variable clock rate, enabling trade-offs between high spectral efficiency and low power/long range.

These concepts are commonly considered complex and challenging for real-time implementation. Therefore, the standard focuses on a minimalistic design defining only absolutely essential functions. This approach led to a lean specification that fits on less than 160 pages. However, so far the specification has not yet been tested to be implementable, especially in real-time. Such validation is crucial to increase confidence in the correctness of the standard and provide real-world performance insights.

The main contributions of this paper are as follows:

- We propose a practical system design for LiFi that aims to support industrial wireless communication based on the active specification in IEEE Std 802.15.13-2023.
- We show how the proposed design can be implemented using open-source software frameworks and custom field programmable gate array (FPGA) logic.
- We validate the basic functionality of the medium access control (MAC) and Pulsed Modulation PHY (PM-PHY) of the new standard through experiments.

The remainder of the paper is structured as follows. Section II introduces the main characteristics of LiFi for Industry 4.0. Section III describes the new IEEE Std 802.15.13-2023 and its MAC and two PHYs. Section IV describes the experimental platform and an exemplary implementation in real-time. Section V describes initial test results in the lab. Finally, the paper concludes with a summary and outlook in Section VI.

II. LiFi for Industry 4.0

A. System concept based on distributed MIMO

Future industrial automation requires robust and efficient wireless data transmission [6], connecting mobile agents, such as humans with handheld devices, AGVs or other automation systems. While existing wireless technologies are constantly evolving, the physical properties of radio propagation fundamentally limit their ability to guarantee real-time transmissions. This is difficult because radio waves penetrate walls, which can result in unpredictable inter- and intra-technology interference from other radio systems [7]. Furthermore, modern cellular campus networks based on private spectrum licenses can provide high QoS but are very costly. The use of industrial, scientific and medical band (ISM) bands is subject to regulatory constraints that set limits on the achievable reliability and latency of the communication protocols.

Light, when used as a communication medium, allows for sharply delimited propagation zones even inside the same room and generally a higher degree of spatial reuse compared to radio waves as light does not pass through walls. Light is unregulated as a wireless medium and thus deployable without limitations on the communication protocols, such as licensing or mandatory coexistence listen-before-talk mechanisms. OWC, relying on intensity-modulated visible or infrared light from light-emitting diodes (LEDs) or laser, could therefore be a valuable complement to the radio spectrum [8], [2].

However, the properties of light also impose design challenges for the communication protocols. Firstly, efficient communication usually requires a free line-of-sight (LOS) between the light emitter and the receiver, as reflections are usually too weak for higher data rates (100 Mbit/s or more). When the LOS is obstructed, communication is typically not possible, or only with much lower data rates (a few Mbit/s) via diffuse reflections. It has been shown previously that leveraging spatial diversity through MIMO with multiple

transmitters and receivers can make communication robust against blockages [1]. Secondly, the small size of optical wireless cells leads to frequent handovers when the user is mobile. While this is not so typical for nomadic applications, e.g., in enterprises, mobile robots in a manufacturing cell or automated guided vehicles in an industrial scenario can indeed be mobile at speeds of more than 1 m/s. Alizadeh Jarchlo et al. [9] investigated the outage duration in an OWC network and show how to reduce the duration down to 200 ms in a system with multiple optical access points (APs) that were connected to a common backhaul network. For industrial applications, this outage needs to be further reduced.

Our proposed design approach to achieve this is to transmit and receive from multiple ceiling-mounted transceivers to and from a single user simultaneously, as depicted in Fig. 2. The coverage areas are designed with considerable overlap between adjacent transmitters and receivers, accordingly. This allows to dynamically adapt the set of transceivers jointly serving all the users, following mobility and enables uninterrupted wireless connectivity. Moreover, signal quality at the cell edge is improved, because interference can be converted into useful signal and blockages can be overcome through redundant LOS links. The advantages of this approach directly address the high reliability and low latency/jitter requirements in industrial applications. In the literature, these concepts are denoted as "joint transmission coordinated multipoint", "cell-free" [10] networks or "D-MIMO." This "user-centric" selection of access points is preferable and can be based on CSI feedback from the mobile devices which is exchanged over the backbone between the access points [11]. In modern "Cloud-RAN" networks [12], this is possible with less complexity, as the analog signals, and thus CSI, are available at the central baseband processor pool.

So far, this concept has been mostly theoretical and only coarsely investigated through initial simulations [2], with little data on the performance in realistic scenarios. Beysens et al. [13] implemented DenseVLC, a cell-free OWC system based on the modified OpenVLC architecture [14]. Complete specification in an appropriate standard, real-time implementation as well as measurements of the user-centric D-MIMO concept were, to the best of our knowledge, not yet investigated. Such work is essential to identify and address major implementation challenges, obtain insights into the performance and pave the way for robust low latency transmission in industrial applications.

B. Industrial communication and time-sensitive networks

Industrial automation continues to enhance the efficiency of modern production processes. Communication is at the core of most industrial automation and multiple proprietary industrial communication protocols have found widespread adoption. Proprietary wired protocols such as PROFINET, EtherCAT, or Sercos are designed to support distributed control systems where cycle times, and thus allowed de-

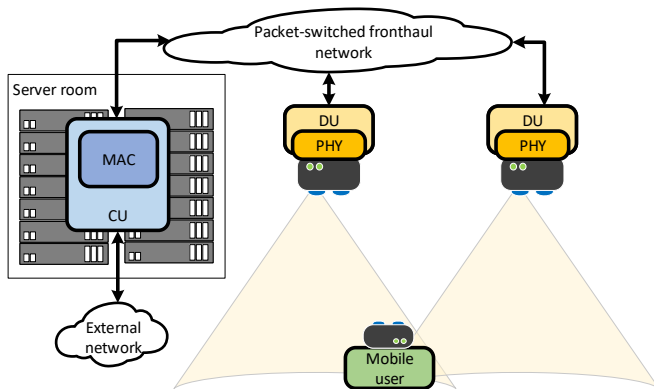


FIGURE 2. Concept for the user-centric OWC system implemented by using a MAC-PHY split between the coordinator and the DUs. Mobile devices move within the coverage area and are served via LOS to one or more DUs [15]

lays and delay variation, can be well below a millisecond [16]. Typical applications are, for example, communication between a sensor and an actuator in a distributed control system. However, whether such demanding applications will be realized wirelessly in the near future is not clear.

Existing technologies for wireless industrial communication include Wireless HART, ISA 1000, Bluetooth, IEEE 802.11, and proprietary modifications thereof. However, these technologies provide only limited real-time capabilities due to their medium access protocols and/or the use of shared radio frequencies, where interference cannot be fully controlled. Lately, cellular networks (5G) have been considered for wireless factory automation. While the aforementioned technologies are based on license-free radio bands, 5G requires licenses for operation. As a benefit, uncoordinated interference from other devices is less likely. However, radio is still prone to interference from malicious transmitters and spurious emissions from other sources.

Over the last years, industrial Ethernet has found widespread interest as a wired technology and was improved to support industrial communication as part of the TSN activity within the IEEE 802.1 and 802.3 working groups. While TSN aims to unify the lower layers of industrial communication networks, OPC Unified Architecture (OPC UA) unifies the higher layers of application protocols. The combination of both breaks up the classical pyramid of automation and is expected to become one of the primary technology stacks for future industrial communication networks [17].

As the IEEE 802.1 TSN standards are not bound to a specific medium, other media than Ethernet can support TSN standards and integrate with TSN-capable LANs in principle. In the future, this could allow industrial network operators to select the suitable (wireless) medium for a given data stream between two automation devices based on the required communication characteristics and available paths. Therefore, diverse communication techniques and media would create a

large toolbox for the realization of heterogeneous industrial communication networks.

III. The IEEE 802.15.13 Standard

A. Recent standards development for LiFi

First standardization activities began almost 20 years ago. The IEEE Std 802.15.7-2011 defines multiple physical layers and a MAC sublayer taken from the latest version of IEEE 802.15.4 at that time. It was revised in 2018, focusing mainly on optical camera communication (OCC), but is not widely implemented.

ITU-T G.9991 [4] is an add-on to the ITU-T G.hn family of standards, which defines fixed home networking for diverse media. G.hn includes multiple sub-standards, to which ITU-T G.9991 adds a specification for light communication. The MAC is based on a flexible TDMA scheme with additional support for shared time slots, specified in ITU-T G.9961. G.9991 defines two physical layers, based on direct current (DC)-biased OFDM (originally specified in ITU-T G.9960) and on asymmetrically clipped OFDM. Due to the commercial availability of G.hn-based chip sets, first LiFi systems became market-ready based on this ITU-T specification.

IEEE Std 802.11bb, an amendment to IEEE Std 802.11 (Wi-Fi) introducing light communication, aims to increase the market size by reducing the chip set cost. It is currently specifying the use of light for the transmission of genuine Wi-Fi signals. The approach is to reuse the existing physical and MAC layers in IEEE Std 802.11 and only define new channels over the light medium without substantial changes to the rest of the standard. The goal is to leverage existing soft- and hardware to enable the fast development of new LiFi devices based on the versatile protocol toolbox that IEEE 802.11 has developed over the years. However, in this way LiFi inherits the drawbacks of Wi-Fi for industrial applications, such as limited robustness in multiuser and multicell environments besides unpredictable latencies and jitter.

B. IEEE Std 802.15.13 Networks

In the process of revising the IEEE 802.15.7 standard [18], a new task group was formed to focus on high data rate communication for specialty applications. The new group, IEEE P802.15.13, focused on reception via photodiodes instead of cameras, allowing higher communication bandwidths. The physical layers of the standard make use of techniques that are similarly used for radio communication and do not rely on specific properties of light as a medium. Instead of radio frequencies, a very low carrier frequency is used and the signals are shifted to the base band between zero and a few hundred MHz. This real-valued base band is then modulated by varying the emission intensity of a LED or laser.

IEEE 802.15.13 networks consist of coordinator and member devices. The coordinator is responsible for the management of the network, e.g., to associate new members

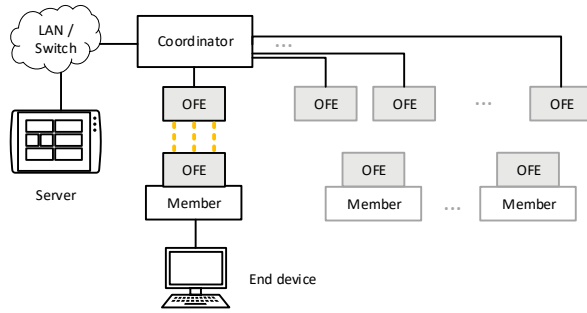


FIGURE 3. Architecture of a 802.15.13 network. The coordinator is attached to the local network and has one or more OFEs that are distributed throughout the coverage area. Members move in the area and are attached to end devices [19].

and coordinate the medium access. The network has a star topology and transmissions occur only between the coordinator and members. Fig. 3 depicts the architecture of IEEE 802.15.13 networks. IEEE 802.15.13 networks allow coordinators to have multiple OFEs and employ MIMO techniques for spatial diversity and parallel transmissions to multiple devices. To support seamless mobility within the coverage area, additional OFEs can be installed to provide coverage for members in a larger area, as indicated in Fig. 3. MIMO operation will be described further in Section 3.

C. IEEE 802.15.13 MAC

In this section, we present the most relevant functions of the MAC sublayer, as specified by the task group.

1) MSDU transmission service

Following the architecture of IEEE 802, IEEE 802.15.13 networks support the MAC service, defined in IEEE 802.1AC. Therefore, the coordinator bridges MAC service data units (MSDUs) based on a source and a destination MAC address between the connected LAN and the end devices associated with each member. Consequently, IEEE 802.15.13 networks can be integrated into existing local area networks. Thus, all IEEE 802.15.13 devices are assigned a 48-bit MAC address. Although multiple techniques in the draft aim to improve reliability and reduce frame losses, as detailed in Section 4, it should be noted that a cable-like QoS cannot be guaranteed. This is due to varying channel and interference conditions caused by the mobility of devices and objects that may block the line-of-sight. This leads to changing link load and link availability and, therefore, time-variant capacities and link availability for each device. Consequently, frames may be lost due to movement, which is, however, a general characteristic of wireless communication. Compared to radio communication, sporadic interference through emitters in the same bands can be greatly reduced due to the more directional transmission and the use of the optical spectrum, which is unlicensed but available many times in parallel at different wavelengths and rarely used for communication so

far. Thus, we can expect the light to behave more cable-like than radio.

2) Medium access

Due to the directional propagation of light, devices are usually unable to sense a busy medium at an intended receiver before transmitting. This is known as the hidden terminal problem in wireless networks that employ carrier sense multiple access (CSMA). To avoid hidden terminal situations, IEEE 802.15.13 networks utilize centrally coordinated medium access for all data transmissions. For that purpose, the coordinator allocates time slots for transmissions to and from member devices in a dynamic TDMA approach. Time in the TDMA scheme is subdivided into successive superframes, as depicted in Fig. 4. Each superframe consists of slots, which are an abstract representation of time used for resource scheduling. The coordinator allocates the available slots to devices for transmission. These dedicated allocations are called guaranteed time slices (GTSs).

The allocation is dynamic to allow reaction to varying conditions, such as time-variance of the channel through mobility and changing traffic requirements in the network. Moreover, the coordinator allocates part of the available superframe slots for random access based on a slotted ALOHA scheme with back-off. Random access is required when a device is not yet associated or needs to request additional transmit resources without using previously allocated GTS. Allocations for random access are referred to as random time slices (RTSs). The scheduling of RTS and GTS for devices determines the real-time characteristics of transmission and is not specified by the standard but is intended to be vendor-specific. After preparing a schedule, the coordinator notifies devices of their GTS and RTS through control frames. Based on their received assignments, devices are free to use their allocated time slots for transmissions without the need to assess the channel state first. While this approach requires all transmitters to be synchronized, it not only avoids the aforementioned issues of carrier sensing, but also alleviates requirements on the fronthaul network used between the central coordinator and the distributed OFEs (D-OFEs), which may have longer delays. Carrier sensing would require bidirectional communication between a coordinator and D-OFEs with very low latency. Digital networking technologies, however, have latencies ranging from multiple tens to hundreds of μ s. For example, modern fronthaul network technologies for cellular networks, such

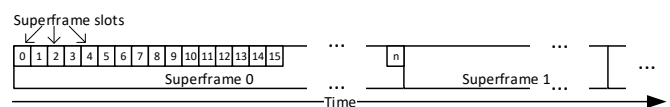


FIGURE 4. Time is subdivided into successive superframes, consisting of n superframe slots each. The superframe number wraps after reaching a value of 65535 [19].

as common public radio interface (CPRI) or Ethernet-based TSN allow delays of up to 100 μ s [20]. Waiting for that time before every transmission would impose significant overhead when performing carrier sensing at each D-OFE before each transmission.

3) Distributed MIMO for mobility support

MIMO is considered a crucial feature of LiFi networks as it alleviates the impact of an interrupted line-of-sight for transmissions through spatial diversity. Support for massive distributed MIMO is a core feature that enables IEEE 802.15.13 networks to cover larger service area with a single coordinator. The current draft includes several functions that allow to implement and operate the coordinator with a scalable number of D-OFEs, as depicted in Fig. 5. The implementation of the fronthaul network is beyond the scope of the standard. Different realizations of the fronthaul network are conceivable, depending on the actual conditions and costs of installation.

To aid the resource scheduling, i.e., assigning time slots and D-OFEs to members, and adapting to mobility and changing channel conditions, the channels between all member OFEs and the D-OFEs of the coordinator are measured as part of a MAC routine. This is indicated by the red and blue arrows in Fig. 5. To achieve this, the standard defines the transmission of explicit MIMO pilot signals as part of physical layer protocol data units (PPDUs) and the provision of successive feedback of the estimated channel state in the reverse link direction. To correlate the feedback with corresponding OFEs, the standard specifies a mapping between MIMO pilot signals and OFE indexes.

Based on the latest channel feedback, coordinators that have multiple D-OFEs can select a suitable subset of D-OFEs for transmission to members, i.e., supporting mobility through antenna selection, forming user-centric virtual cells. Hence, no handover between coordinators is required and transmissions can continue regularly within the same TDMA scheme. Consequently, it is possible to avoid jitter during mobility.

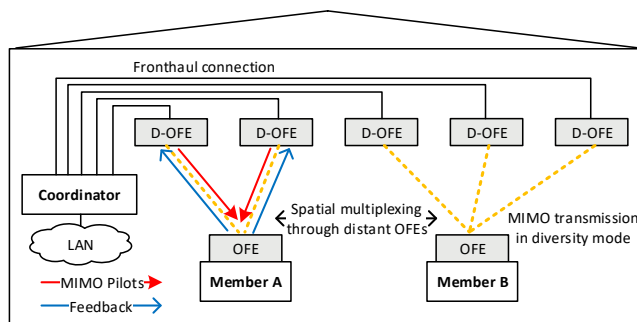


FIGURE 5. MIMO operation in IEEE P802.15.13. Periodic channel estimation through pilot signals and feedback of channel state feedback support transmit diversity, spatial multiplexing and mobility [19].

The use of virtual cells and transmit diversity, i.e., transmitting the same signal from multiple D-OFEs to a receiver in multiple-input single-output (MISO) mode is transparent to the member devices. The effective MISO channel is compensated at the receiver by fast equalization of the channel based on implicit pilots embedded into the PPDUs. Since the logical association with a single

All supported physical layers include a cyclic prefix for block-based frequency-domain-equalization. The variable length allows for a maximum delay spread in the order of several hundreds of nanoseconds. In this way, the synchronicity requirements of transmitters are relaxed so that it is possible to connect D-OFEs to the coordinator via digital technologies like Ethernet, where the time synchronization of D-OFEs is achieved, e.g., via IEEE 802.1AS. When multiple OFEs are present at the coordinator, the standard allows allocating the same TDMA superframe slots to multiple members that “see” different OFEs. This is useful for devices which are covered by different OFEs and thus can be served simultaneously, i.e., without interference. Based on the feedback of channel state information, as described before, the coordinator is able to manage the potential interference between concurrent transmissions to allow this way of spatial multiplexing between members efficiently.

4) Increasing reliability

Several techniques in the draft aim to improve the provided QoS by reducing frame loss, duplication and out-of-order delivery. For example, sequence numbers are added to data frames and allow reordering and elimination of duplicates at a receiver, before data is handed up to the higher layer. An acknowledgment mechanism specifies how receivers can acknowledge frames through either single- or block acknowledgments. Both methods perform a delayed acknowledgment, as immediate acknowledgment would potentially be delayed through a larger delay on the fronthaul network. Lost frames are retransmitted after a configurable timeout. To adapt the data rate and thus robustness of the transmission, devices can transmit requests for certain data rates to prospective transmitters. This allows to signal the maximum supported data rate, depending on the channel conditions. Through explicit signaling, the rate adaptation does not rely on losing frames first, which improves frame loss rates. A fragmentation mechanism allows efficient use of transmit time resources as well as reducing frame loss probability in challenging channels. Aggregation of multiple higher layer data frames can increase efficiency and thus throughput in applications like video streaming. Lately, a mechanism was added that specifies relaying of frames between the coordinator and a member through another member device. This potentially allows to increase throughput, when channel conditions between the relaying device and the coordinator, as well as between the relaying device and the target device

are better than the direct link from the coordinator to the target device.

D. Physical layers

Currently, the draft specifies two physical layers that serve two complementary goals. This effectively serves the conditions in both directions of transmission, downlink and uplink. As mobile devices may have battery and transmission power constraints, energy-efficient modulation is crucial.

On the other hand, the infrastructure part of the network is typically connected to the grid for power supply. Therefore, deployments may use the energy-efficient PM-PHY, presented in Section 1, for the uplink from mobile devices to the coordinator, and the spectrally efficient HB-PHY, presented in Section 2, for downlink transmissions from the coordinator to mobile members.

The physical layers in the standard are frame-based, meaning that analog signals can be transmitted discontinuously. Physical layer frames are referred to as PPDU. Their generic structure is depicted in Fig. 6. A preamble at the start of each PPDU allows receivers to detect a transmission and synchronize with the transmitter. The header includes information about the subsequent fields, such as the structure of optional pilots or the modulation and coding of the payload. Based on that information, receivers are able to demodulate and decode the rest of the PPDU and forward the contents of the payload to the MAC for further processing.

1) PM-PHY

The PM-PHY, where “PM” stands for “pulsed modulation”, is based on OOK modulation and Reed-Solomon forward error correction coding. The OOK has a low peak-to-average power ratio (PAPR), enabling efficient use of energy to extend reach and operate at low signal-to-noise ratios (SNRs) [21]. To remove possible DC-component from emitted signals, 8b10b encoding is applied after scrambling the data. A cyclic prefix (CP) allows block equalization with blocks of 5.12 μs length at a receiver for the support of challenging channel conditions or when multiple OFEs are used for MIMO and the delay spread becomes large.

While the light medium typically only leads to small delay spread through its short range, longer delay spreads may arise through imperfect synchronization of different implementation approaches of the fronthaul network as described in Section 3. To cover those, multiple CP lengths between 1280 μs and 160 μs are defined. The transmitter structure is depicted in Fig. 7.

The PPDU’s header is always transmitted at a symbol rate of 12.5 MHz, while the payload supports higher symbol rates

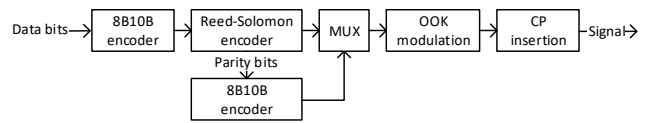


FIGURE 7. PM-PHY transmitter structure. Data is 8b10b-coded against low frequency components. Subsequently, it is FEC-encoded, modulated and blockwise cyclically extended [15].

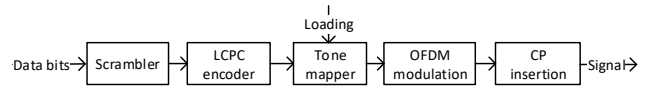


FIGURE 8. HB-PHY transmitter structure. Data is first scrambled and low-density parity-check code (LDPC)-encoded and subsequently OFDM-modulated [15].

of 25, 50, 100, and 200 MHz and thus higher data rates. The PM-PHY was thoroughly evaluated in [21].

2) HB-PHY

The HB-PHY is based on DC-biased OFDM modulation and low-density parity-check code (LDPC) forward-error correction. After scrambling and forward error coding of the input data stream, the coded bits are mapped onto subcarriers of the OFDM signal. The tone mapper allows unequal loading of bits per subcarrier, i.e., so-called “bit-loading.” This is highly beneficial for utilizing LED-based optical frontends efficiently, which exhibit low-pass characteristics [22]. The standard allows loading of 1 to 12 bits per subcarrier. For subcarriers that are less attenuated, a higher number of bits can be loaded, increasing the effective usage of the bandwidth. Fig. 8 depicts the transmitter structure.

The HB-PHY is mostly compatible with the physical layer specified in ITU-T G.9960 [23], which was already successfully tested for light communication [1]. However, in order to adapt to the architecture of the IEEE 802.15.13 standard, information in the header was changed and only a subset of the functionality is supported below the so-called alpha reference point in [23]. The HB-PHY currently supports the bandwidths and data rates of 50, 100, and 200 MHz and 530, 1084 and 2192 MBit/s.

E. TSN support

Since industrial networks are the focus area of application, support of specific standards from TSN in conjunction with IEEE 802.15.13 is a goal of the task group. In addition to being interoperable with IEEE 802.1 LANs, i.e., supporting the transmission service described in Section 1, IEEE 802.15.13 networks need to support the implementation of selected TSN standards in combination with IEEE 802.15.13 compliant devices. Note that TSN standards are individual standards on their own and must be implemented by the vendor of a given device. However, the underlying trans-



FIGURE 6. Packet-based physical layer PPDU format [15].

mission technology, here IEEE 802.15.13, needs to provide fundamental tools to implement a given TSN standard.

Two of the most relevant standards are IEEE 802.1AS, which is a generalized form of precision time protocol (PTP), and IEEE 802.1Qbv for scheduled traffic [24]. For the support of time synchronization over IEEE 802.15.13, the MAC-internal time reference may be used, which synchronizes all devices for medium access. Moreover, the scheduling of resources through the coordinator is not specified within P802.15.13 and the transmission order of MSDUs within a device is unspecified. Thus, time-aware scheduling can be implemented as part of a device as specified in IEEE 802.1Qbv. In this way, basic support of TSN and timely transmission of data frames can be provided. Improved performance, e.g., through even better synchronization at the MAC level and thus improved accuracy for time synchronization or specific improvements to support the implementation of more TSN standards with IEEE 802.15.13 networks can be added through amendments to the standard in the future. Requirements imposed by other TSN standards on IEEE 802.15.13 networks are currently under investigation.

F. Main achievements of 802.15.13

This section provided an overview of the IEEE Std 802.15.13-2013 for wireless industrial communication via light. The standard aims to promote interoperability of devices that form a light-based cellular network to cover larger areas like factory floors. At the core of the specification is a dynamic time division multiple access (TDMA)-based medium access control (MAC) protocol that supports deterministic transmission of data frames. Multiple measures, such as distributed multiple-input multiple-output (MIMO) in a spatial diversity mode, with support of spatial multiplexing of users, frame retransmissions, and relaying aim to increase the reliability of transmissions. Two physical layers support energy- and spectral efficiency and are foreseen to be used in an asymmetrical implementation for the down- and uplink between the coordinator and members, respectively. The standard supports elementary requirements of time-sensitive networking (TSN). Additional functionality may be added to the standard in the future through amendment projects. For example, LiFi allows high precision positioning via the line-of-sight propagation and high bandwidths. Support for the required positioning routines and interfaces could add value through IEEE 802.15.13 networks in the future. Dedicated support for further functionalities from the TSN family of standards is considered crucial for the further development of the standard, albeit its requirements on the standard are still under investigation. With the foreseen set of features, the IEEE 802.15.13 standard aims to add a new physical medium and its distinctive communication characteristics to the toolbox of modern IEEE 802.1-based industrial networks.

IV. D-MIMO Proof-of-Concept

The goal of our proof-of-concept implementation is to validate the feasibility of scalable D-MIMO based on the IEEE 802.15.13 standard and gain performance insights on a practical real-time implementation. Next, we present the design and our implementation thereof.

A. Design

For our D-MIMO approach, we consider a coordinator implementation with a split between MAC and PHY, as known from cellular networks, see Fig. 2. The coordinator's MAC implementation resides in a so-called central unit (CU), while the PHY resides in one or more distributed units (DUs). The CU is connected to one or more DUs and forwards PHY service data units (PSDUs) for downlink transmissions to them and receives PSDUs from them upon successful uplink reception. This central control of transmissions allows for D-MIMO operation with relatively low complexity compared to when CSI needs to be exchanged between APs that participate in a transmission. Applying that concept from cellular networks to OWC with its high number of cells per area was also proposed, e.g., by Kizilirmak et al. [25].

Inspired by the use of digital network technologies to transport fronthaul data in cellular networks, we investigate the use of Ethernet networks to connect the CU and DUs. Compared with dedicated analog lines for each DU, this approach makes networks easy to install and scalable, as the statistical multiplexing gain of packet-switched networks is leveraged. Additionally, this architecture makes it possible to implement the MAC as a virtual function on ordinary server hardware, as long as it has an Ethernet network interface, allowing it to run, e.g., in an existing server room.

B. Implementation

We implemented a minimal setup of the system described in the last section to obtain an initial performance assessment. The system includes a PHY implementation for use as part of the DU and mobile unit (MU), as well as a MAC implementation of the fundamental protocol routines of the coordinator and the mobile device, residing in the CU and MU, respectively. Below, we describe the recent state of our ongoing proof-of-concept implementation.

1) Physical layer implementation

We implemented the PM-PHY from IEEE Std 802.15.13 on a Zedboard with a Xilinx Zynq 7020 FPGA. We connected a 250 MSPS Analog Devices analog-to-digital converter (ADC) and a variable gain amplifier (VGA) via the FMC connector for reception (see Fig. 9 and 10). The PHY implementation supports most of the PHY's operating modes, specifically, the clock rates 12.5, 25, 50 and 100 MHz, leaving out 200 MHz due to resource constraints on the FPGA and the limited ADC sample rate. The PHY receives one transmit vector (TXVECTOR) per transmission through an direct memory access (DMA) interface, containing the

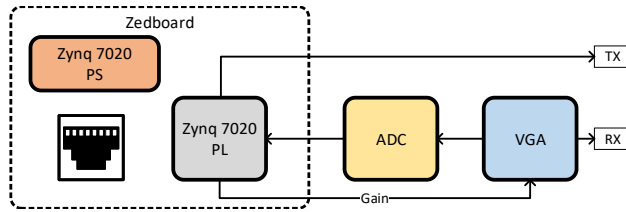


FIGURE 9. Block diagram of the custom hardware used for the DU and MU. The PHY is running on the Zynq 7020 PL (FPGA). The Zynq 7020 PS (ARM CPU) runs the software stack of either the DU or MU [15].

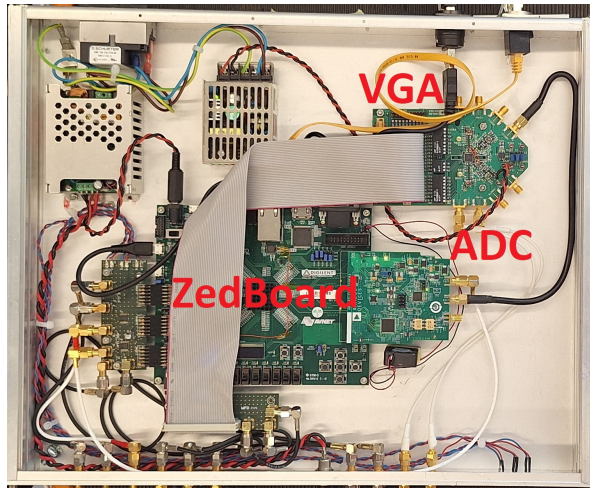


FIGURE 10. The extended Zedboard hardware, used as a DU and MU in the system. A programmable VGA and a ADC, connected via FMC, are mounted with the Zedboard in a 19 inch housing.

PSDU and all necessary parameters to assemble the PPDU. The generated header and the payload/PSDU are scrambled and encoded in 8b10b line code and Reed-Solomon FEC. The preamble, channel estimation symbols, and the MIMO channel estimation symbols are retrieved from a read-only memory (ROM). After modulation and frame assembly, all parts of the PPDU are concatenated and buffered for transmission. Since the signal consists of ON/OFF levels only, no digital-to-analog converter (DAC) is necessary and the signal is directly outputted via the Pmod pins. Fig. 11 depicts the main building blocks of the transmitter FPGA design.

In the receiving direction, the PHY receives samples from the ADC and detects the frame based on correlation with the known preamble. The VGA's gain is controlled through an automatic gain control (AGC) core that analyzes the received signal strength during the frame start. To set the gain quickly, the AGC core is connected with the VGA through a parallel interface. An frequency domain equalization (FDE) equalizes the header blocks based on the coefficients obtained from the header channel estimation field. It then demodulates the OOK signal and performs FEC decoding. The demodulation clock rate, scrambler initialization, and cyclic prefix length for the payload are obtained from the demodulated header and the receiver pipeline is reprogrammed for payload demodulation. If the payload is modulated at a higher clock

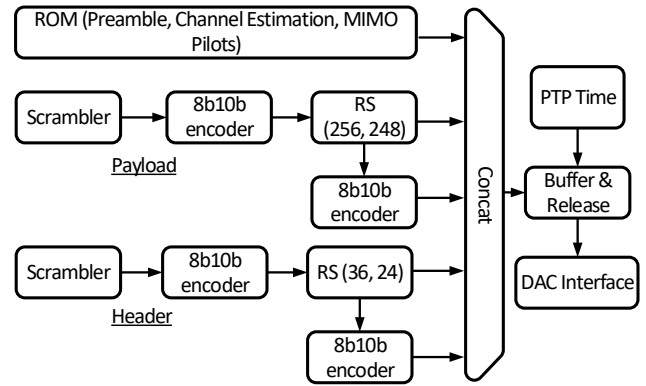


FIGURE 11. Block Diagram of the PM-PHY transmitter implementation [15].

rate than the header, the FDE coefficients are updated based on the payload channel estimation field of the PPDU. Successfully decoded PSDUs are forwarded via the receive interface.

2) IEEE 802.15.13 MAC software implementation

We implemented a minimal feature set of the 802.15.13 MAC in the coordinator, as well as in the mobile devices to allow transfer of Ethernet frames over the optical link. The coordinator's MAC is running as a userspace application on a standard Linux Ubuntu server, constituting the CU with the help of the Data Plane Development Kit (DPDK) framework. DPDK allows bypassing the kernel for networking functions and thus creating highly parallelized userspace networking applications [26]. The coordinator receives frames from the Ethernet ports of the CU server, encapsulates them in the IEEE 802.15.13 frame format and forwards them to the DUs for transmission based on the MAC protocol rules. Vice versa, it receives encapsulated Ethernet frames from the DUs upon uplink reception and forwards them to the Ethernet ports connected with an external network after MAC processing.

The MAC features of the mobile device are implemented as a kernel module for Linux, running on the ARM core of the Zynq 7020 system-on-a-chip (SoC). The software stack receives uplink Ethernet frames from the Zedboard's network interface, encapsulates them, and transmits them in the assigned TDMA slots, passing them to the PHY implemented on the co-located FPGA. Conversely, it receives downlink frames from the PHY and forwards them to the Ethernet port after extraction from the MAC frame.

3) System with MAC-PHY-Split

We integrated the PHY and MAC implementation in a system setup that acts like a bridge, i.e., passing Ethernet frames between the CU's and the MU's Ethernet ports. In the overall system, the CU is connected to the DUs through an

TABLE 1. PHY data rates for each of the tested clock rates [28].

Clock Rate (MHz)	Data Rate (Mb/s)
12.5	8.99
25	17.41
50	32.94
100	59.43

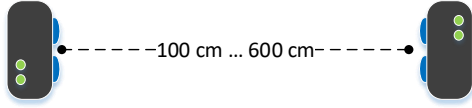


FIGURE 12. Simplified experimental point-to-point topology with a transmitter and a receiver. The two OFEs are facing each other at a distance varying between 100 and 600 cm [15].

Ethernet switch. In our experimental system, we use a CTC Union IGS-1608SM-SE with PTP and SyncE functionality. The switch’s integrated PTP master synchronizes the CU and all DUs to a common reference time. The coordinator software runs on a 10-core Xeon server central processing unit (CPU), using 8 cores for the data path in a pipeline architecture. We use the Ethernet clock signal to operate the time module within the DU to improve accuracy as described in [27].

Our DUs include a simple software to receive TXVECTORS from the fronthaul network and forward them to the PHY via DMA. A time-trigger in the FPGA enables the transmission of PPDU based on the synchronized PTP time. The MU is based on the same hardware as the DU but runs different software on the two ARM cores, implementing parts of the MAC protocol on the mobile device side.

V. Experiments

A. PM-PHY SISO Performance Experiment Setup

Previously, Hinrichs et al. [21] evaluated the PM-PHY in offline experiments. Therefore, an evaluation based on a real-time implementation is the logical next step. As a basis for future system-level performance evaluation, we conducted initial performance tests of our real-time PHY implementation through point-to-point SISO measurements

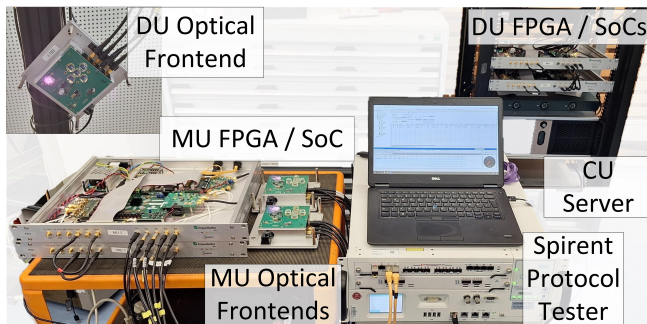


FIGURE 13. The measurement setup with one CU, one DU, and two MUs in our laboratory.

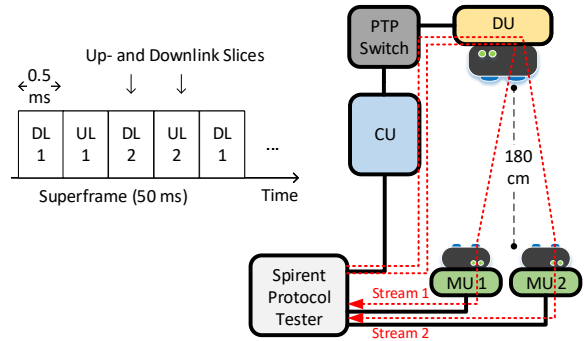


FIGURE 14. The experimental setup and MAC schedule for the multiple-user measurements. Two MUs are served by a CU with one DU. The TDMA schedule assigns slices of 500 slots (0.5 ms) to each MU for downlink and uplink in a round-robin fashion.

over variable distances. We set up one transmitter and one receiver, consisting of the extended Zedboard hardware, in the laboratory, as depicted in Fig. 12. Both are connected to custom-designed LED-based OFEs through coaxial cables, carrying the differential analog signal. The OFEs, designed and built by Fraunhofer HHI, are mounted on tripods at a height of 1.8 m above the ground. We transmitted frames and measured the packet error rate (PER) while varying the distance between 100 and 600 cm. We performed 10k frame transmissions for each of the four supported modulation and coding schemes (MCSs) (12.5 MHz, 25 MHz, 50 MHz, and 100 MHz) as well as for three different PSDU (i.e., payload) sizes of 100, 400, and 1400 bytes. The net data rates for the maximum PSDU size, considering the overhead from the PPDU header, are listed in Table 1. For each transmission, the receiving PHY attempted to demodulate and decode the PPDU in real-time and notified the software about erroneous frames.

B. PM-PHY SISO Performance Results

The results show that our implementation supports real-time data transmission with all tested MCS and payload sizes. Fig. 15 depicts the PER versus distance for all combinations. For larger payloads, the PER is higher, which is a common effect since more bits lead to more potential bit errors. For the PSDU size of 100 bytes, only the MCS with a clock rate of 50 and 100 MHz lead to significant packet errors at higher distances. All lower-rate MCSs can cover distances up to 600 cm with a relatively low PER. Note that the maximum distance is typical for communication between the ceiling and the shop floor in a manufacturing hall. For larger PSDUs, however, the error probability increases with distance and results in significant packet loss for 25 MHz and 50 Mhz clock rates at higher distances as well. In addition to previous simulations and offline experiments, the results show for the first time that the PM-PHY from 802.15.13 is implementable in real-time on an FPGA. While its design is kept simple, it offers moderate data rates that are sufficient to reliably transport short control frames, e.g., in automation systems.

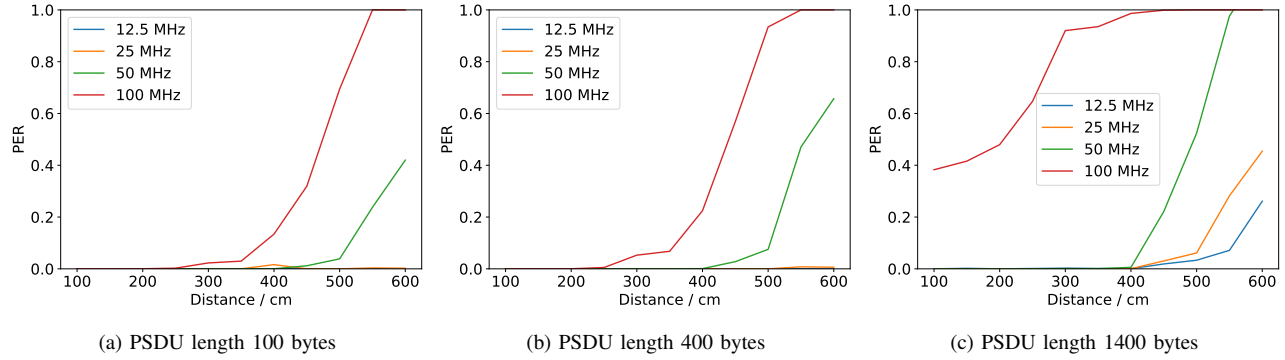


FIGURE 15. SISO PHY PER over distance for the PSDU lengths 100, 400 and 1400 bytes and clock rates 12.5, 25, 50, and 100 MHz [15].

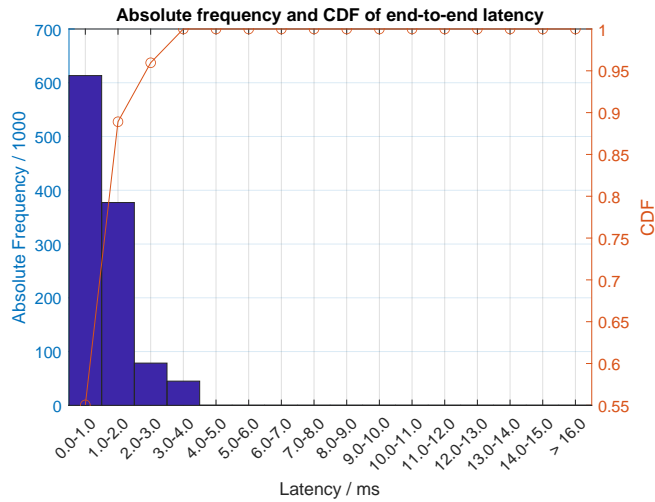


FIGURE 16. Absolute frequencies and CDF for the measured latency of both streams. The maximum observed latency is 3.9 ms.

C. MAC Multiple-Access Performance Experiment Setup

After validating the PHY performance, we proceed to validate the basic function of the MAC in the downlink direction. We set up a system consisting of a coordinator, residing in our CU, and a D-OFEs, implemented in our DU and connected to the DU through an Ethernet network as described in 3. We set up two member devices, based on our MU FPGA hardware, around 1.8 m below the DU, as shown in Fig. 14.

A simple round-robin scheduler in the CU was configured for a TDMA with a 50 ms superframe duration and 0.5 ms (i.e., 500 slots) long slices. For duplexing, each MU received one uplink and one downlink slice successively. Thus, each MU was served every 2 ms in the downlink and every 2 ms in the uplink direction. We configured the Coordinator to use MCS 1, i.e., 25 MHz clock rate for transmissions with the PM-PHY. A Spirent protocol tester was connected to the CU and both MUs. It transmitted two data streams with 100 packets per second, 1 million packets in total, each having a payload of 100 bytes to the CU. The CU processed the frames, determined the transmit time

according to the MAC schedule, and forwarded them to the DUs for transmission. After reception at the MU, the latency of frames was measured at the protocol tester. Fig. 13 shows the setup in our laboratory.

D. MAC Multiple-Access Performance Results

The results show that no frames exceeded a latency of 3.9 ms (see Fig. 16). Therefore, the CDF does not exhibit a long tail like typical radio communication. This is due to the absence of interference in the light channel and the deterministic TDMA-based medium access. However, although the transmitted frame rate is a multiple of the schedule slot duration, we still observed latency variation. This is due to the fact that we did not synchronize our MAC with the actual source of the data. In TSN networks, this is done so that packets do not have to wait in queues for too long. In our case, the timing between the sender and our 802.15.13 network drifted, causing some packets to wait during the uplink time slices, leading to a higher delay. In a system with full TSN support, the scheduler would be aware of the incoming periodic streams and could accommodate them in the medium access schedule accordingly. Moreover, we observed latency outliers up to 18 ms for higher packet rates. This is due to the fact that we did not yet fully exhaust the possibilities to operate the CU and MU with real-time capabilities. Thus, other processes running on their CPUs preempted the data-processing, leading to latency spikes.

We conclude that OWC and the IEEE 802.15.13 standard are fundamentally suitable for real-time data transmission. To achieve the full potential, however, measures from the TSN suite of standards must be implemented.

VI. Conclusion and Outlook

We presented our concept for optical wireless communication as a suitable wireless technology for modern industrial networks. As a basis for such development, we proposed to make use of the recently approved IEEE Std 802.15.13 and gave an overview of its features. Moreover, we described our current activities in implementing a prototype of that standard based on freely available hardware, i.e., standard

servers and FPGA development boards. Our prototype is designed to enable distributed MIMO transmission through multiple ceiling-mounted frontends that are centrally connected through a packet-based fronthaul network.

We observed that our FPGA-based PHY implementation of the IEEE 802.15.13 PM-PHY is capable of transmitting and receiving data over 600 cm at different clock rates. As per its low complexity specification, our PM-PHY implementation thus achieves around 17 Mbit/s over six meters and 60 Mbit/s over four meters while covering a large area. We also demonstrated that the system was able to transmit two low data rate streams reliably with bounded latency below 4 ms to multiple receivers. These fundamental results indicate the suitability of the medium light for real-time wireless transmission and that the techniques specified in the newly approved standard can be used. To increase the performance, further techniques from the TSN suite of standards should be implemented, e.g., to synchronize the communication system with the rest of the network and support isochronous data streams.

Future work might include an evaluation of the OFDM-PHY from IEEE Std 802.15.13, which provides higher spectral efficiency. Moreover, we aim to investigate data transmissions with multiple cells covering a larger area and mobility of multiple users.

REFERENCES

- [1] P. W. Berenguer, P. Hellwig, D. Schulz, J. Hilt, G. Kleinpeter, J. K. Fischer, and V. Jungnickel, "Real-time optical wireless mobile communication with high physical layer reliability," *Journal of Lightwave Technology*, vol. 37, no. 6, pp. 1638–1646, 2019.
- [2] K. L. Bober, S. M. Mana, M. Hinrichs, S. M. Kouhini, C. Kottke, D. Schulz, C. Schmidt, R. Freund, and V. Jungnickel, "Distributed multiuser mimo for lifi in industrial wireless applications," *Journal of Lightwave Technology*, vol. 39, no. 11, pp. 3420–3433, 2021.
- [3] S. M. Kouhini, C. Kottke, Z. Ma, R. Freund, V. Jungnickel, M. Müller, D. Behnke, M. M. Vazquez, and J.-P. M. G. Linnartz, "Lifi positioning for industry 4.0," *IEEE Journal of Selected Topics in Quantum Electronics*, vol. 27, no. 6, pp. 1–15, 2021.
- [4] International Telecommunication Union, "High-speed indoor visible light communication transceiver - system architecture, physical layer and data link layer specification," ITU-T Rec. G.9991, Geneva, Switzerland, Tech. Rep., 2021, international Telecommunication Union.
- [5] "Ieee standard for information technology–telecommunications and information exchange between systems local and metropolitan area networks—specific requirements part 11: Wireless lan medium access control (mac) and physical layer (phy) specifications amendment 6: Light communications," *IEEE Std 802.11bb-2023 (Amendment to IEEE Std 802.11-2020 as amended by IEEE Std 802.11ax-2021, IEEE Std 802.11ay-2021, IEEE Std 802.11ba-2021, IEEE Std 802.11az-2022, IEEE Std 802.11-2020/Cor 1-2022, and IEEE Std 802.11bd-2023)*, pp. 1–37, 2023.
- [6] M. Luvisotto, Z. Pang, and D. Dzung, "High-performance wireless networks for industrial control applications: New targets and feasibility," *Proceedings of the IEEE*, vol. 107, no. 6, pp. 1074–1093, 2019.
- [7] A. Seferagić, J. Famaey, E. De Poorter, and J. Hoebeker, "Survey on wireless technology trade-offs for the industrial internet of things," *Sensors*, vol. 20, no. 2, p. 488, 2020.
- [8] Y. Almadani, D. Plets, S. Bastiaens, W. Joseph, M. Ijaz, Z. Ghassemlooy, and S. Rajbhandari, "Visible light communications for industrial applications—challenges and potentials," *Electronics*, vol. 9, no. 12, p. 2157, 2020.
- [9] E. A. Jarchlo, E. Eso, H. Doroud, A. Zubow, F. Dressler, Z. Ghassemlooy, B. Siessegger, and G. Caire, "Fdma: A novel frequency diversity and link aggregation solution for handover in an indoor vehicular vlc network," *IEEE Transactions on Network and Service Management*, vol. 18, no. 3, pp. 3556–3566, 2021.
- [10] E. Nayebe, A. Ashikhmin, T. L. Marzetta, and H. Yang, "Cell-free massive mimo systems," in *2015 49th Asilomar Conference on Signals, Systems and Computers*, 2015, pp. 695–699.
- [11] R. Zhang, J. Wang, Z. Wang, Z. Xu, C. Zhao, and L. Hanzo, "Visible light communications in heterogeneous networks: Paving the way for user-centric design," *IEEE Wireless Communications*, vol. 22, no. 2, pp. 8–16, Apr. 2015.
- [12] A. Checko, H. L. Christiansen, Y. Yan, L. Scolari, G. Kardaras, M. S. Berger, and L. Dittmann, "Cloud ran for mobile networks—a technology overview," *IEEE Communications Surveys & Tutorials*, vol. 17, no. 1, pp. 405–426, 2015.
- [13] J. Beysens, Q. Wang, A. Galisteo, D. Giustiniano, and S. Pollin, "A cell-free networking system with visible light," *IEEE/ACM Transactions on Networking*, vol. 28, no. 2, pp. 461–476, 2020.
- [14] Q. Wang, D. Giustiniano, and D. Puccinelli, "Openvlc: Software-defined visible light embedded networks," in *Proceedings of the 1st ACM MobiCom workshop on Visible light communication systems*, 2014, pp. 15–20.
- [15] L. Bober, A. Ebmeyer, J. Andree, F. Dressler, and V. Jungnickel, "Optical wireless for industrial communication: Practical results using ieee std 802.15.13: (invited paper)," in *2024 IEEE International Conference on Communications Workshops (ICC Workshops)*, 2024, pp. 945–949.
- [16] M. Wollschlaeger, T. Sauter, and J. Jasperneite, "The future of industrial communication: Automation networks in the era of the internet of things and industry 4.0," *IEEE Industrial Electronics Magazine*, vol. 11, no. 1, pp. 17–27, 2017.
- [17] D. Bruckner, M.-P. Stănică, R. Blair, S. Schriegel, S. Kehrer, M. Seewald, and T. Sauter, "An introduction to opc ua tsn for industrial communication systems," *Proceedings of the IEEE*, vol. 107, no. 6, pp. 1121–1131, 2019.
- [18] "Ieee standard for local and metropolitan area networks—part 15.7: Short-range optical wireless communications," *IEEE Std 802.15.7-2018 (Revision of IEEE Std 802.15.7-2011)*, pp. 1–407, 2019.
- [19] K. L. Bober, E. Ackermann, R. Freund, V. Jungnickel, T. Baykas, and S.-K. Lim, "The ieee 802.15.13 standard for optical wireless communications in industry 4.0," in *IECON 2022 – 48th Annual Conference of the IEEE Industrial Electronics Society*, 2022, pp. 1–6.
- [20] "Ieee standard for local and metropolitan area networks – time-sensitive networking for fronthaul," *IEEE Std 802.1CM-2018*, pp. 1–62, 2018.
- [21] M. Hinrichs, J. Hilt, V. Jungnickel, S.-K. Lim, I. S. Jang, J.-D. Jeong, and M. Noshad, "Pulsed modulation phy for power efficient optical wireless communication," in *ICC 2019 - 2019 IEEE International Conference on Communications (ICC)*, 2019, pp. 1–7.
- [22] P. W. Berenguer, V. Jungnickel, and J. K. Fischer, "The benefit of frequency-selective rate adaptation for optical wireless communications," in *2016 10th International Symposium on Communication Systems, Networks and Digital Signal Processing (CSNDSP)*, 2016, pp. 1–6.
- [23] Int. Telecommun. Union, "Unified high-speed wireline-based home networking transceivers system architecture and physical layer specification," ITU-T Rec. G.9960, Geneva, Switzerland, 2015.
- [24] "Ieee standard for local and metropolitan area networks – bridges and bridged networks - amendment 25: Enhancements for scheduled traffic," *IEEE Std 802.1Qbv-2015 (Amendment to IEEE Std 802.1Q-2014 as amended by IEEE Std 802.1Qca-2015, IEEE Std 802.1Qcd-2015, and IEEE Std 802.1Q-2014/Cor 1-2015)*, pp. 1–57, 2016.
- [25] R. C. Kizilirmak, O. Narmanlioglu, and M. Uysal, "Centralized light access network (c-lian): A novel paradigm for next generation indoor vlc networks," *IEEE Access*, vol. 5, p. 19703–19710, 2017.
- [26] Linux Foundation, "Data plane development kit (DPDK)," <http://www.dpdk.org>, 2015. [Online]. Available: <http://www.dpdk.org>
- [27] A. Ebmeyer, K. L. Bober, M. Hinrichs, and V. Jungnickel, "Fronthaul synchronization requirements for distributed mimo in lifi systems," in *2024 IEEE Wireless Communications and Networking Conference (WCNC)*, 2024, pp. 1–6.
- [28] "Ieee standard for multi-gigabit per second optical wireless communications (owc), with ranges up to 200 m, for both stationary and mobile devices," *IEEE Std 802.15.13-2023*, pp. 1–158, 2023.